Palacký University Olomouc
Faculty of Science

Department of Experimental Physics

Differential and homodyne detection of light

Bachelor's Thesis

Matúš Frick

Palacký University Olomouc
Faculty of Science

Department of Experimental Physics

Differential and homodyne detection of light

Bachelor's Thesis

Author:	Matúš Frick
Study programme:	B1701 - Physics
Field of study:	Applied Physics
Form of study:	Full-time
Supervisor:	RNDr. Miroslav Ježek, Ph.D.

Thesis submitted on: .....

Univerzita Palackého
Přírodovědecká fakulta

Katedra experimentální fyziky

Diferenciální a homodynní optická detekce

Bakalářská práce

Autor: Matúš Frick
Studijní program: B1701 – Fyzika
Studijní obor: Aplikovaná fyzika
Forma studia: Prezenční
Vedoucí: RNDr. Miroslav Ježek, Ph.D.

Práce odevzdána dne: .....

Abstract

In this Thesis, I perform a detailed characterization of the basic quantum pulsed homodyne detector. I characterize the charge sensitive amplifier, the photodiodes and required optical setup. I execute the calibration to the vacuum state and I detect the quantum noise of light. I verify the linearity and other properties of the detector such as electric noise, bandwidth. Furthermore, I create a quantum random number generator using homodyne detector. Random bits are extracted from the measured quantum noise with the rate of 4 Mbit/s and verified using DIEHARDER battery of tests.

Keywords

`Homodyne detection, Quantum detection, Quantum detectors, Photodetector`

Acknowledgments

I would like to express the deepest appreciation to my supervisor and advisor RNDr. Miroslav Ježek, Ph.D., his hard work accompanied by excitement and knowledge inspired me. Without his guidance and persistent help, this Thesis would not exist. In addition, I thank Mgr. Michal Dudka for manufacturing and assembly of the amplifier printed circuit board. I would like to thank my parents, my girlfriend and all my friends who supported me during my studies.

Matúš Frick

Declaration

I hereby declare that I have written this Bachelor's Thesis—and performed all the presented research and experimental tasks—by myself, while being supervised by RNDr. Miroslav Ježek, Ph.D. I also state that every resource used is properly cited. I agree with the Thesis being used for teaching purposes and being made available at the website of the Department of Optics or Department of Experimental Physics.

Signed in Olomouc on ....

Matúš Frick

Contents

Chapter 1

Introduction

1.1 What is homodyne detection

The homodyne detection is a widely used technique for finding the information encoded in the amplitude and the phase of unknown signal. The unknown signal is compared to the signal with a defined phase/frequency/amplitude known as the local oscillator. This technique can be used with any electromagnetic signal. Firstly, it was used in RF communication. We will use it for optical signals. The term homodyne means that the frequency of the local oscillator and unknown signal is the same (in contrast to different frequencies in heterodyne detection). Also, the local oscillator and unknown signal must be coherent, they are typically derived from the same light source. The unknown signal and the local oscillator interfere in an interferometer and the output signals are detected. Balanced homodyne detection was firstly applied in frequency domain. In our case, the homodyne detector is designed for measurements in time domain. The signal and the local oscillator are provided by a pulsed laser. This time domain pulsed regime is necessary for measurement of the non-classical features of light, such as multiphoton states localized in particular times. The measurement of quantum states is highly demanding. There are some challenges that need to be solved beforehand. The electronic noise of the detector must be smaller than the quantum noise of optical states of light. There is a need for fast components, faster than the repetition of the pulsed signal. Also, there is a need for photodiodes with good quantum efficiency.

The requirements are hard to fulfil and we cannot use a commercial detector, so we have to construct home-made one. There are only two types of amplifiers used in quantum optical homodyne detectors which can be used in the pulsed regime. Both types allow for electronic noise smaller than quantum noise. The first one uses a combination of a low-noise FET transistor and a charge sensitive amplifier. After the first amplification, the signal is shaped with shaping amplifiers. The second type uses one operational amplifier in the trans-impedance configuration. In our detector, we use the charge sensitive amplifier. The trans-impedance amplifier scheme is newer and faster. The charge sensitive amplifier was used in the beginning of the quantum homodyne detection. Balancing is easier with a charge sensitive amplifier and also its signal to noise ratio is typically higher than for trans-impedance amplifier.

Table 1.1: Comparison between various homodyne detectors, taken from [5]. CS stands for charge sensitive, TI stands for trans-impedance.

Characteristics	[3] (2000)	[6] (2002)	[4] (2008)	[7] (2009)	[5] (2011)	This work (2019)
Wavelength (nm)	790	786	1064	800	791	810
3 dB bandwidth (MHz)	1	50	250	54	100	2
Clearance (dB)	14	5	7.5	12	10-18	> 23
Amplifier	CS	-	-	TI	TI	CS

1.2 State of the art

The first homodyne detection for quantum optical used in frequency domain was performed by Slusher et al. in 1985 [1]. They detected optical squeezed states. For the quantum state reconstruction with applications in hybrid quantum information processing, homodyne detection in time domain is needed. Using quantum tomography one can obtain Wigner's function, containing full information about the quantum state of light. The first quantum homodyne detector which works in time domain was constructed by Raymer et al. [2] in 1993. First fast detector with a bandwidth of 1 MHz was created by Hansen et al. [3] in 2001 who used charge sensitive amplifier in the well-known electronic scheme used for nuclear and particle physics. Many homodyne detectors are based on the Hansen's charge senstive detector. Fastest homodyne detector was created by Okubo et al. [4] in 2008 with 3 dB bandwidth of 250 Mhz. This detector was not stable and had a small clearance in comparison with others. Kumar et al. [5] made significant improvement developing a detector with bandwidth around 100 MHz and with fairly good clearance. The detectors made by Zavatta et al. [6], and Haderka et al. [7] should be also mentioned. Various implementations of homodyne detectors and their key parameters are summarized in Tab. 1.1. Namely, the bandwidth and signal to electronic noise (clearance) are compared. Homodyne detection was used for conditional preparation and characterization of various strongly non-classical optical signals. For example, Ourjoumtsev et al. [8] in 2006 used a homodyne detector for detection of cat states. There are many applications of homodying in quantum information processing and quantum metrology. Homodyne detection can also be used as a quantum random number generator [9].

1.3 Outline

In this work, I will describe how our homodyne detector is made, how the photodiodes are chosen, how the detector is calibrated for the vacuum state of light, how quantum noise is measured and how the results of the quantum noise measurement are used as a quantum random number generator. In the chapter 2, I will explain the fundamentals of homodyne detection. Also the basic terms will be clarified. The essential scheme of developed homodyne detector is shown there. In the chapter 3, I will describe our charge sensitive amplifier. I will explain how I measure the parameters of the homodyne detector, such as gain, noise and response. The scheme of the measurement setup will be in this chapter. In the chapter 4, I will discuss the parameters of the photodiodes, for example the response and quantum efficiency. I will describe the process of photodiode matching and the selection of the best photodiode pair which will be

used. In the chapter 5, I will explain the optical setup with all the components. Also, I will comment on calibration to the vacuum state and how I found the linear region of the detector. The extraction of random bits from the quantum noise of light will be described in this chapter. Result of the randomness testing could be found in appendix.

Chapter 2

Fundamentals of homodyne detection

In classical physics the state of the light could be approximately described with one complex variable α represented by one point in the phase diagram. This complex number, α has a real part q and an imaginary part p,termed quadrature amplitudes. These two parts are then

$$q = \frac{1}{\sqrt{2}}(\alpha + \alpha^*), \tag{2.1}$$

$$p = \frac{1}{i\sqrt{2}}(\alpha + \alpha^*). \tag{2.2}$$

The angle

$$\phi = \arctan\frac{p}{q}, \tag{2.3}$$

represents the optical phase. The norm of α is the overall amplitude of the state. Squared amplitude is equal to the intensity I of the signal in classical optics. In quantum physics, this number corresponds to the mean photon number,

$$|\alpha|^2 \sim I \sim \langle N \rangle. \tag{2.4}$$

Vacuum state of light containing no photons would be one point in the zero. In full quantum description, however, the light is modelled as quantized harmonic oscillator and therefore the Heisenberg principle is applied. The light is not anymore described with one point in the phase space but it is represented using uncertainty areas. Heisenberg uncertainty principle tells us that

$$\Delta q \Delta p \geq \frac{1}{4}, \tag{2.5}$$

for the vacuum state the uncertainties are $\Delta q = \Delta p = 1/2$, shown in Fig.2.1 (a). The same goes for coherent states of light, shown in Fig.2.1 (b). If the state is squeezed then $\Delta q \neq \Delta p$. This uncertainty manifests itself as quantum noise.

The basic scheme of the homodyne detection is visualized in Fig. 2.2. In balanced homodyne detection, an unknown signal is mixed with the known signal of the local oscillator. An unknown signal and the signal of local oscillator

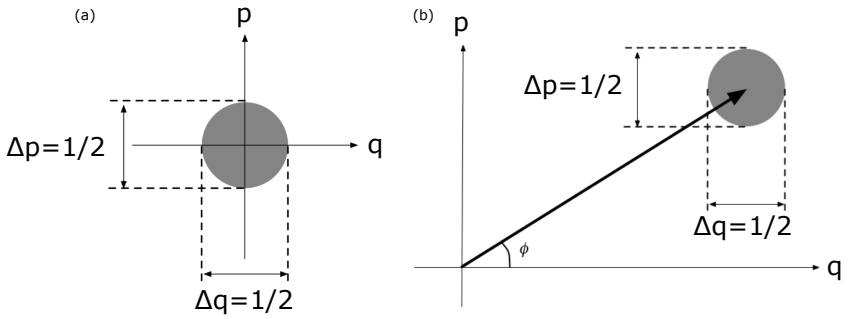

Figure 2.1: (a) Phasor diagram for a vacuum state. (b) Phasor diagram for a coherent state.

needs to be coherent. The signals interferes and are divided on the 50 % beam-splitter into two output signals. These signals have the same intensity. We want them to be as similar as possible. Then these two signals are brought on the photodiodes, where the optical signal is converted into an electric photocurrent. The photocurrents from both photodiodes are subtracted. The differential photocurrent is

$$I = (N_\alpha - N_{\mathrm{LO}}) \cdot (T - R) + 4\sqrt{R \cdot T \cdot N_{\mathrm{LO}}}\, Q(\phi) + o(N_{\mathrm{LO}}, U_{\mathrm{bias}}, U_{\mathrm{noise}}, \ldots), \quad (2.6)$$

where N_α is the mean photon number of the measured signal, N_{LO} is the mean photon number of the local oscillator, R, T are coefficients of reflection and transmission of the beam splitter and $o(\ldots)$ contains the parasitic elements such as electric noise and others. We want this error element to be as small as possible. $Q(\phi)$ quadrature is defined as $Q(\phi) = q\cos\phi + p\sin\phi$. The values of this function depend on the angle ϕ, which describes the angle of the measured state in phase diagram with respect to the local oscillator. When we scan values of the quadratures for $\phi = \langle 0, 2\pi \rangle$ we can reconstruct the full information about the measured quantum optical state. We can measure Wigner's function of this state. If the spiltting ratio is $R = T = 1/2$ and we assume that the detection is perfect, the Eq. 2.6 will transform to

$$I \sim \sqrt{N_{\mathrm{LO}}} \cdot Q(\phi). \quad (2.7)$$

Final differential photocurrent after subtraction is amplified and shaped, as shown in Fig. 2.2 by a simplified schematic of charge-sensitive amplifier. We can detect the output signal in the time domain with the oscilloscope or in the frequency domain with the spectrum analyzer. In our detector, the R/T ratio can be almost perfect but an error element will always be there. There are many problems, such as the differences between the two photodiodes and the noise generated by the amplifier. Well designed and precisely adjusted charge sensitive amplifier is important for a good balancing in homodyne detection.

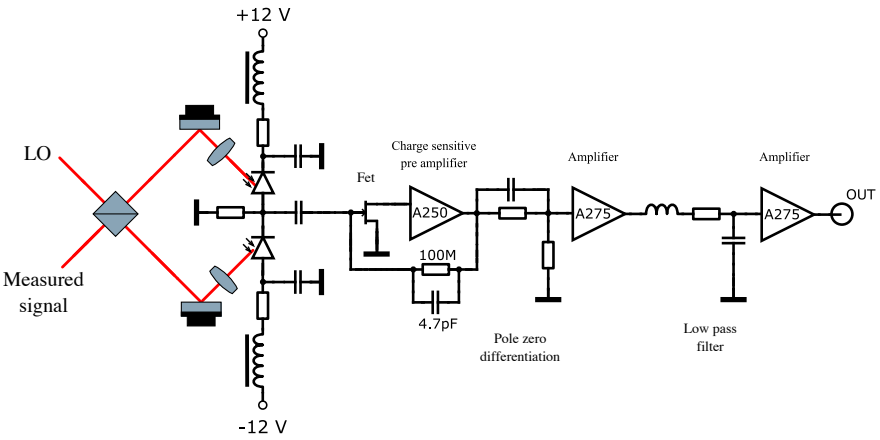

Figure 2.2: The simplified schema of our homodyne detection.

Chapter 3

Charge sensitive amplifier

Well designed and well-made electronic amplifier is crucial part of good homodyne detector. Our charge sensitive amplifier follows the well-known scheme, which is widely used for detection in nuclear physics with one detector. H. Hansen et al. [10] were the first, who used this scheme for optical homodyne detection. This scheme of the detector was chosen because of its low noise. The printed circuit board and assembly of our amplifier was performed by M. Dudka based on the design provided by M. Ježek. Same as Hansen et al., we used a slightly modified scheme of the amplifier which is in the datasheet of amplifier AMPTEK A275. Our implementation of charge sensitive amplifier was thoroughly tested without photodiodes. I measured the gain of the amplifier, linearity, and electronic noise, which must be smaller than quantum noise. Also, I measured the shape of output pulses and I described the time response of the amplifier.

3.1 Characteristics of amplifier

Gain g of the charge-sensitive amplifier is defined as a ratio of output pulse voltage peak U_{out} and input charge Q_{in}. The gain was measured using the scheme 3.1 (a). The input signal was prepared using the signal generator (Tektronix AFG3252) which generates a square wave with frequency $f = 1$ MHz. The amplifier responds to both negative and positive edges of the test signal. The generator is connected to a small capacitor of $C = 2.7$ pF. This capacitor converts the input voltage to the charge $Q_{\text{in}} = U_{\text{in}} \cdot C$ expressed as number of electrons. The capacitor was used only during the measurement of the characteristic of the homodyne detector. After this measurement, the capacitor was replaced with larger capacitor with capacity of 470 pF. During all measurements, the voltage $U = \pm 12$ V was applied to the amplifier. Output signal was measured in the time domain with a 200 MHz oscilloscope (Hameg 2024).

At the output, there are negative and positive pulses, see Fig. 3.1 (b). I measured the difference between the maximum and the base line of these pulses for positive pulses. For the negative pulses I measured the difference between the minimum and the base line. This differences are called an output voltage. The function of the output voltage on the input charge is a linear function in a specific interval, see Fig. 3.1 (c). The function is perfectly linear between

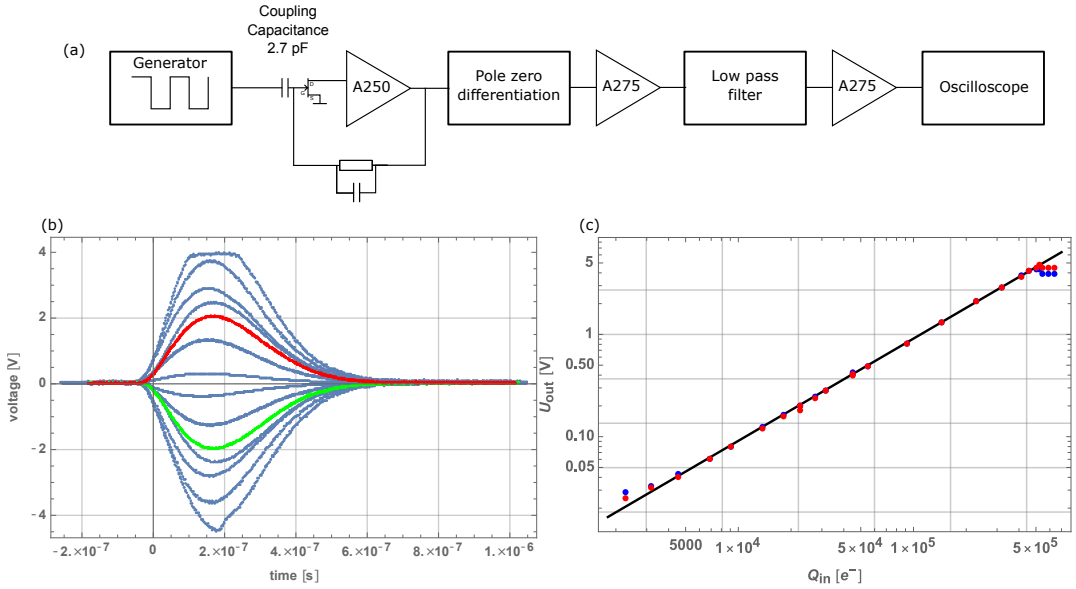

Figure 3.1: (a) The scheme of aperture which was used for measuring the gain and the pulses in time domain. (b) Output pulses of amplifier in time domain. Normal pulses and pulses in saturation. (c) Gain and linearity of the charge sensitive amplifier. There are two types of output voltage (red points are voltage of positive pulse peak and blue ones of negative).

8000 electrons and $5{\cdot}10^5$ electrons. The reasons why the respose function is not linear outside of this region are the noise of the amplifier and its saturation. The electronic noise is larger than the weak output signal and the pulses are lost within. The saturation can be seen for large values of the output voltage. The amplifier works well in the linear area. Gain is a slope of the linear part of the curve in Fig. 3.1 (c). The function of the fit is

$$U_{\text{out}} = g \cdot Q_{\text{in}}. \tag{3.1}$$

The gain is $g = 9.1 \;\; \mu\text{V/e}^-$.

The time response of the amplifier is measured in the same way as I measured the gain, Fig. 3.1 (a). We want the amplifier to have the same characteristic as for the positive so for the negative pulses. I measured and compared two pulses which have the same input voltage but opposite polarity, see Fig. 3.1 (b). The compared pulses are the red one and the green one. I describe the pulses with the full width at half maximum (FWHM), the duration of the rise and the decay tails. The rise time and decay time are measured from 10 % to 90 % of the amplitude. The response of the positive (red) pulse with amplitude $A = 2.08$ V is $t^{\text{red}}_{\text{FWHM}} = 270$ ns, $t^{\text{red}}_{\text{rise}} = 126$ ns and $t^{\text{red}}_{\text{decay}} = 276$ ns. The response of the negative (green) pulse with amplitude $A = -2.06$ V is $t^{\text{green}}_{\text{FWHM}} = 264$ ns, $t^{\text{green}}_{\text{rise}} = 122$ ns and $t^{\text{green}}_{\text{decay}} = 262$ ns. The rise time is nearly the same for both pulses. The difference in measured decay times is caused by the difficult reading of the values. In future measurements of time response I would suggest to use averaging functionality of an oscilloscope. The amplitude and the gain are the same for positive and negative pulses in the linear interval. Positive pulses

saturate at voltage 3.89 V. The response and shape of the pulse are the same for negative and positive pulses below this voltage.

The scheme of **the noise** measurement is Fig. 3.2 (a). For measuring the noise I turned off signal generator. The amplifier was still connected to a power supply. I used cursors on the oscilloscope to measure the difference between maximum and minimum noise voltage. With this window I measured noise $U_{\mathrm{p2p}} = 20$ mV. This value corresponds to the value of six stadard deviations, so called sigma. One sigma is $U_{\mathrm{noise}} = 3.3$ $\mathrm{mV_{rms}}$. After dividing this value with gain we get $Q_{\mathrm{noise}} = 363$ $\mathrm{e^-}$. For the second measurement of noise I used electronic spectrum analyzer (Rohde and Schwarz) instead of the oscilloscope. During the measurement, the amplifier was connected to the power supply with a voltage of $U = \pm 12$ V. When the amplifier was connected to the generator with its signal output turned off, the analyzer showed a spectrum with multiple peaks. This means that there is another source of noise, probably produced by the generator or by the electromagnetic interference. For that reason, the amplifier was connected only to the power supply and spectral analyzer during the measurement (the tektronix generator was disconnected). In this case, the result was a smooth spectrum, see Fig. 3.2 b).

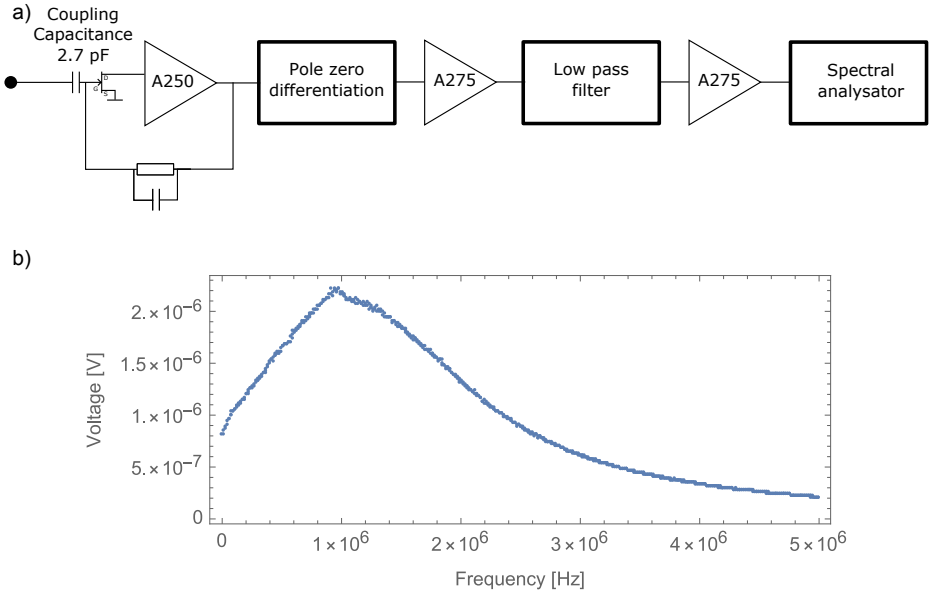

Figure 3.2: (a) The scheme of the system used for measuring the noise of the amplifier. At the input nothing is connected. (b) Noise of the amplifier measured on a spectrum analyzer.

From measured data we can calculate the total noise power as

$$P = \int_0^{\nu_{max}} \mathrm{Var}[U(\nu)]\ \mathrm{d}\nu, \tag{3.2}$$

where ν is frequency, P is the total noise power and $Var[U(\nu)]$ is variance of voltage signal $U(\nu)$. I numerically calculated the integral of variances $P = 7.3 \times 10^{-6}$ $\mathrm{V^2}$. Square root of this number is standard deviation of normal distribution

of noise voltage $U_{\text{noise}} = 2.7\ \text{mV}_{\text{rms}}$. Which gives us value of $Q_{\text{noise}} = 297\ \text{e}^-$. This value is smaller than the result which I got from measurement with an oscilloscope. Noise from the signal generator could cause this difference between the two values. Also, I performed the first noise measurement with the amplifier case not closed sufficiently. With an open enclosure, it receives a lot of signals and noise as it behaves like an antenna. Consequently, every measurement of the noise should be conducted with a metal case of the amplifier closed. I summarize all the measured parameters of our charge sensitive amplifier in Tab. 3.1.

Table 3.1: The parameters of the charge sensitive amplifier.

	Measured parameters
Gain	9.1 $\mu V/e^-$
Noise	297 electrons
t_{FWHM}	270 ns
t_{rise}	126 ns
t_{decay}	262 ns

Chapter 4

Photodiodes

The photodiodes convert optical signal into an electric current. In homodyne detection scheme, two photocurrents are subtracted. For that reason, we want to have the photodiodes with the same response. We use Si-PIN diodes S3883 produced by Hamamatsu, which possess the optimal trade-off between efficiency, capacitance and the response speed. These photodiodes are widely used for homodyne detection. Hansen et al. [3], Ježek et al. [7], Windpassinger et al. [11] use this type of photodiodes in their detectors. The manufacturer claims that these photodiodes have the cutoff frequency of 300 MHz, and quantum efficiency 92.2 % at wavelength 780 nm. The maximal reverse voltage is 30 V, the active diameter is 1.5 mm, the spectral response is between 320-1200 nm with a sensitivity peak at 840 nm.

We had 6 pieces of these photodiodes. The goal was to chose the best pair to be soldered onto the board of the amplifier. For finding the best pair we used pulsed laser signal from Toptica femtosecond laser. Pulse length was smaller than 300 fs. This laser is used because the response of the photodiode is not influenced by the shape of the laser pulse. The laser pulses are so short that they can be described as a Dirac delta function with respect to the photodiode bandwidth. The photodiodes were tested one at a time under the same conditions. Each photodiode was connected to the testbed, which was made according to the scheme 4.1. The photodiode was biased with a power supply with the voltage U_{bias}. The testbed was designed to minimize noise of this voltage, using sequence of low pass filters in the bias arm. The signal from the photodiode was read by an oscilloscope (LeCroy 1.5 GHz). This setup was used for the measurement of the photodiode response. The shape of the pulse for every photodiode can be found in Fig. 4.2 (a).

In homodyne detection, the amplitude of two pulses could be compensated by changing the splitting ratio of the beamsplitter or by attenuation of laser signals in front of the photodiodes. Also, the position of the pulse in time can be varied by changing the length of the path of the beam. This is the reason why I was numerically changing the amplitude and shifting the pulses in time during the comparison. I compared the shape of pulses using the overlap parameter

$$O = \int_0^{\mathrm{T}} |\mathrm{U}_1(\mathrm{t}) - A \cdot \mathrm{U}_2(\mathrm{t} + B)| \, d\,\mathrm{t}. \tag{4.1}$$

This parameter is used because it characterizes the quality of the subtraction in

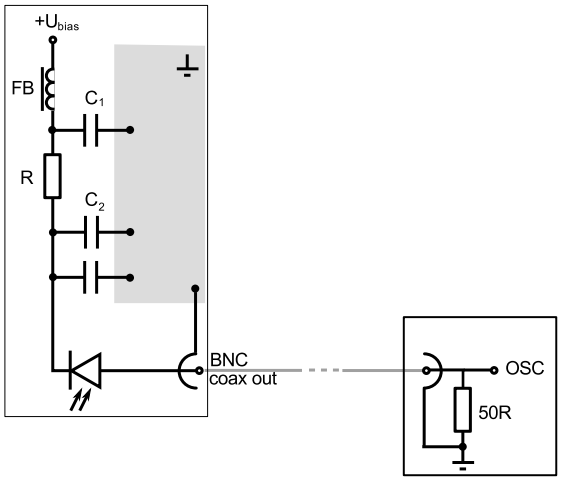

Figure 4.1: The scheme of the testbed for the photodiode characterization.

the homodyne detector. The parameter A scales the amplitude U_2 of the pulse and B moves $U_2(t)$ in time. I compared the pulse for each photodiode with all the other photodiodes. Value A is taken between $\langle 0.8, 1.2 \rangle$ and B is from -20 samples to 20 samples from the initial position. The first photodiode and the fourth photodiode form the most similar pair, see Fig. 4.2 (b).

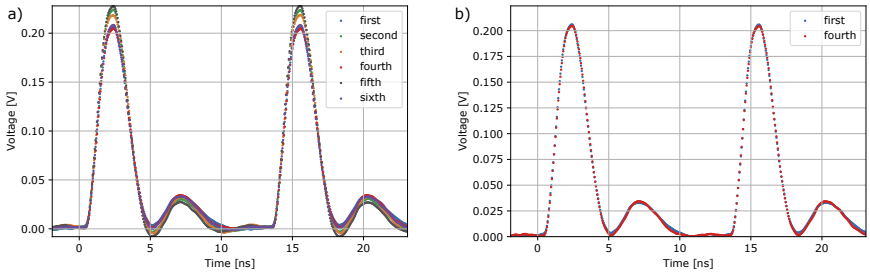

Figure 4.2: (a) The time response of all the measured photodiodes. (b) The response of the best pair of the photodiodes with $A = 1$ and $B = 0$.

The shape of photoelectric pulses depends on the bias voltage U_{bias} of the photodiodes and the polarization, focus and the other parameters of incident optical pulses. The sensitivity to the U_{bias} is shown in Fig. 4.3 (a). For a better understanding of how the response depends on U_{bias}, the area under the pulse versus U_{bias} is visualized in Fig. 4.3 (b). This area is linearly increasing with U_{bias}. We can see that the shape of the pulse is changing with the value of bias voltage. That means we can use U_{bias} for a slight modification of the shape of the pulse.

I also measured the dependence of quantum efficiency on incident light polarization. The beam impinges photodiode under the angle of 45°. The polarization of the beam was changing from horizontal to vertical, see Fig. 4.4 (a). The best

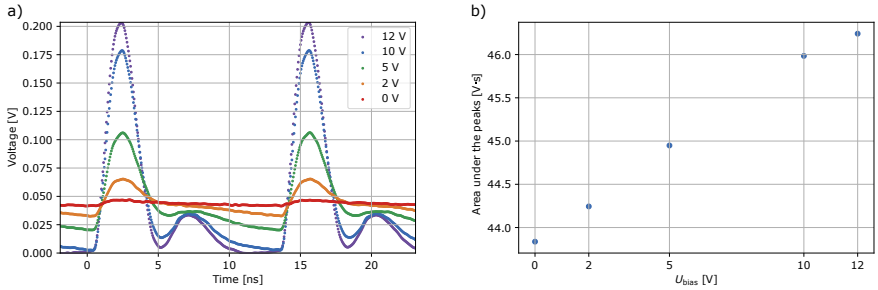

Figure 4.3: (a) The dependence of the photodiode response on bias voltage. (b) The area under the pulse versus U_{bias}.

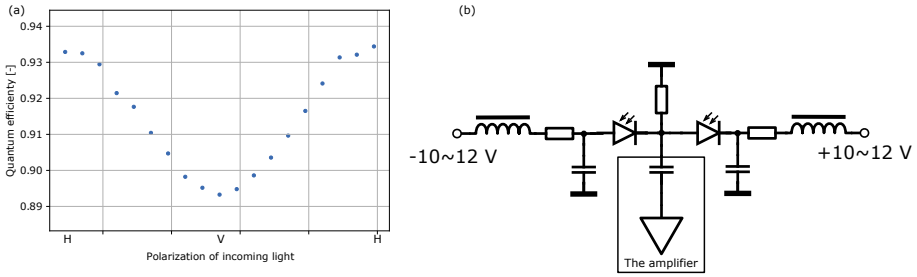

Figure 4.4: (a) Quantum efficiency versus polarization of incoming light. Maximum is for horizontal polarization. (b) The scheme of the connection of photodiodes before the amplifier.

quantum efficiency is measured for horizontally polarized signal. This efficiency is taken for the calculation of detector efficiency. I measured the maximum quantum efficiency of 93.3 % at 775 nm. We can reach even better quantum efficiency if we remove the glass from the photodiode cover. The detector will be used mainly for wavelengths 800 nm and 810 nm, where the efficiency of the photodiodes is slightly higher.

Two photodiodes were selected for the developed homodyne detector. U_{bias} applied on the photodiodes can be modified using precise ten turns potentiometers. Before photodiodes, we attached low pass filters, see Fig. 4.4 (b). They attenuate high frequencies of the bias voltage and reduce the noise.

Chapter 5

Calibration of homodyne detection

5.1 The optical setup for calibration of homodyne detector

For optical vacuum state calibration, we used the optical setup shown in the Fig. 5.1. The pulser was connected to the laser diode, so the signal from the laser diode was in the form of the nanosecond pulses with the repetition frequency of 1 MHz. The laser diode was manufactured by QPhotonics QFLD-808-50S-PM and emits a wavelength of 808 nm. The oscilloscope trigger was set on the signal from the pulser.

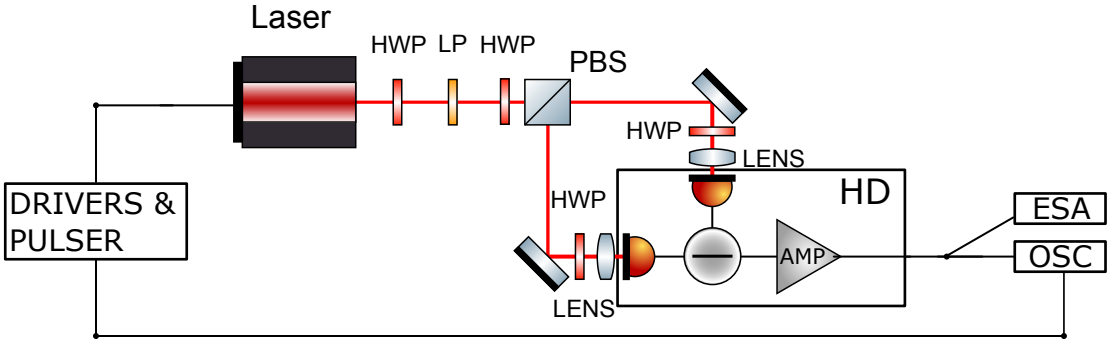

Figure 5.1: The optical setup for calibration of homodyne detector. HWP half-wave plate, LP linear polarizer, PBS polarizing beam-splitter, ESA electronic spectrum analyzer, OSC oscilloscope. This setup was used for measurement of different powers of local oscillator.

The optical signal from laser diode impinges the half-wave plate and the linear polarizer. Both are mounted in manual rotation mounts. With this combination of the half-wave plate and the linear polarizer, we got defined polarization of laser beam. With the rotation of the half-wave plate, it is possible to set continuously the power of the signal (attenuation is possible). The signal

continues to the next half-wave plate and after that to the polarizing beam-splitter. With this half-wave plate in precise rotation mount, we can change splitting ratio of the beam splitter, which is crucial for balancing of homodyne detector. The transmitted and reflected parts have different polarization. One has vertical and one horizontal polarization. For that reason, the two signals are brought to the half-wave plates. The polarization of one signal was changed to match the polarization of the second signal. These half-wave plates can be used for a little change of quantum efficiency of photodiodes. The signals are focused to at photodiodes. These photodiodes are mounted into the detector case under the angle of 45 °. The quantum efficiency is better if the incoming signal does not land on the photodiode upright but under the angle. The first, rough balancing is made with the half-wave plate in precise manual rotation mounts right before the beam-splitter. With this plate, we roughly set the R/T ratio. For a precise setting of R/T ratio, we can use half-wave plates which are situated in the setup after beam-splitter. The additional configuration of focus may be needed for better balancing. The setting of U_{bias} is used for precise balancing. Usually, the decreasing the U_{bias} makes the pulse wider, see Fig. 4.3 (a).

5.2 The data processing

Approximate balancing can be made using an oscilloscope. On the oscilloscope, we brought a trigger signal from the pulser and signal from the homodyne detector. We want the pulses from the homodyne detector as balanced as possible, see Fig. 5.2 (a). For more precise balancing, we connect the output from the detector to the spectral analyser, see Fig. 5.2 (b). In unbalanced detection, there should be peaks Fig. 5.2 (b) blue trace. This trace has a peak at 1 MHz. This peak corresponds to the repetition rate of the laser diode. The second peak at 2 MHz corresponds to the second harmonic oscillation of the laser. With better balance, the peaks will be smaller. If the detector is balanced, it detects the quantum noise. In this case, the peaks are not visible, as shown in Fig. 5.2 (b) orange trace. With the setting of U_{bias}, we can minimize also higher harmonic frequencies. The electronic noise is measured with no input, Fig 5.2 (b) green trace. We measured the noise in the dark room as it is sensitive enough to detect stray light from monitors, room lighting and other sources.

We detect pulses on an oscilloscope and visualized them one over other, see Fig. 5.3 (a) and Fig. 5.4 (a). These two traces are plotted for the different power of local oscillator. We integrate the small neighbourhood of the maximum of the pulse. This integration is equal to quadrature Q'. We can make a histogram of these quadratures. We find the mean of this distribution and subtract it from every Q': $Q = Q' - \langle Q' \rangle$. This subtraction is possible because we know that the offset is caused by the amplifier. After the subtraction, we have got a new distribution which is symmetric around the zero point. These quadratures in time-domain without offset are visualized in Fig. 5.3 (b), Fig. 5.4 (b) and the histograms are in Fig. 5.3 (c), Fig. 5.4 (c). The histogram represents the distribution of fluctuation of quadratures of vacuum state of light in time. This distribution is normal distribution and therefore can be fitted with Gauss function and variance can be read from the fit.

We measured these distributions for different values of power of local oscil-

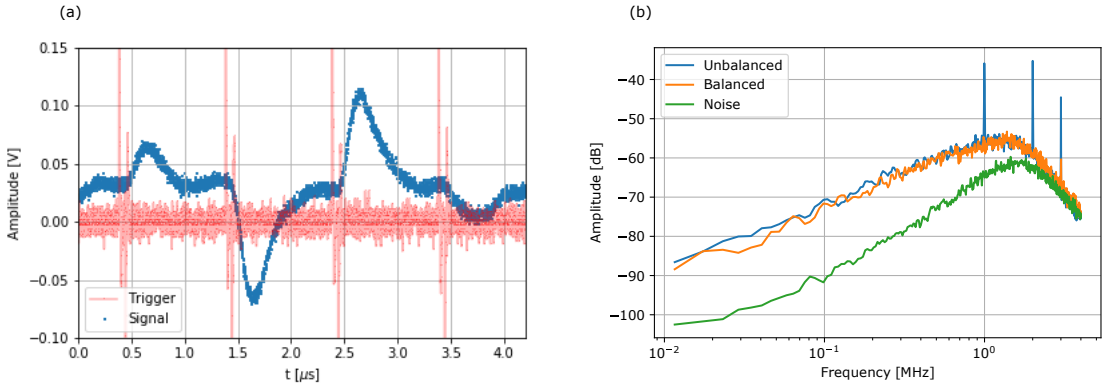

Figure 5.2: (a) Balanced homodyne detection measured on oscilloscope. Red signal is trigger signal from pulser. This signal is larger than the vertical axis range. Blue signal is signal from balanced homodyne detector. (b) Ilustrating image of the output of homodyne detection on the electronic spectrum analyzer. The green trace is the electronic noise, the orange trace is the result of balanced homodyne detection, the blue trace (with peaks) represents unbalanced detection.

lator. The variance is proportional to the power of local oscillator. We plotted this dependence in Fig.5.5. We fitted the measured values with linear function.

$$Var = a \cdot N_{\mathrm{LO}}, \tag{5.1}$$

with $a \approx 2.2 \times 10^{-6}$ V·μs^{-2}. Our detector works properly only in the linear interval. The linear interval is between 1 mio-100 mio photons in the local oscillator pulse. The higher powers are not longer in the linear region. This could have various reasons. For example, the laser is not stable, we changed the focus of the laser on the photodiodes for larger values (it was impossible to balance the detector without the change of the focus), the detector could be saturated. The linear region is important because we need to chose the point where we fix the operating power of the local oscillator in here. The criteria for choosing the working point are the high stability of the balancing and the high clearance, i.e. the high signal to electronic noise ratio. After fixing the power of local oscillator we will measure again the distribution of the quadratures. The unknown signal will be measured with the same power of the local oscillator and will be shifted to zero mean and rescaled by the standard deviation of the previously measured vacuum state (with no signal). The maximum clearance of our homodyne detection is more than 23 dB, shown in Fig. 5.5. For the higher values of clearance, the detector starts to be unstable.

5.3 Quantum random number generator

Our first application of the homodyne detection is a quantum random number generator. The quadrature amplitude is a random quantity [9]. The quadrature histograms from the section 5.2 can be divided around zero into two parts with the same probability of finding a quadrature value there. We can assign

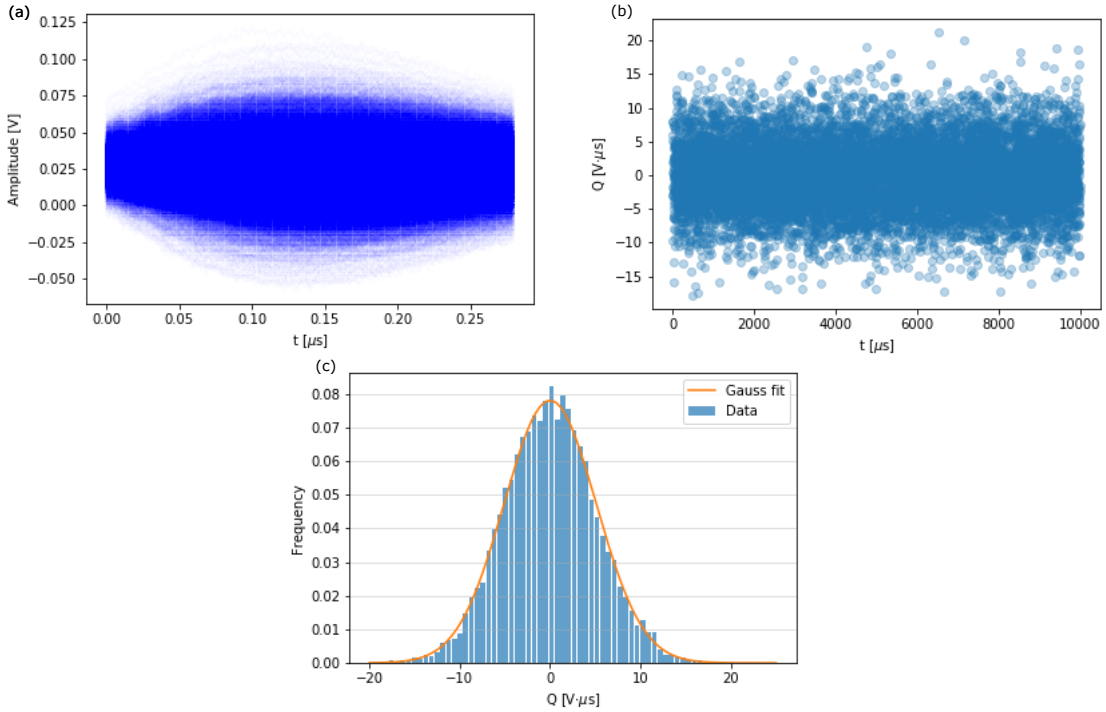

Figure 5.3: Results of measurement with power of local oscillator $N_{LO} \approx 5$ mio photons in the entry. (a) Every pulse of the one measurement visualized one over another. (b) The amplitude of quadratures visualized over time. (c) Histogram made from quadratures, fitted with Gauss distribution.

value zero to the negative quadratures and value one to the positive ones. With this logical conditions we create the random number generator. This generator produces 1 Mbit/s of random bit rate, which can be further increased. The quadrature of histogram quantum vacuum state of light posses normal distribution. The range $\langle 0 : 1 \rangle$ of the corresponding cumulative distribution function is divided into the equidistant parts. The boundary values for normal distribution are obtained using the inverse function applied to the border values of the equidistant parts of the range. Normal distribution is transformed in such way in the uniform distribution if the number of the equiprobable parts goes in limit into the infinity. To every part, we assign a binary number. The amount of random numbers depends on the amount of the parts. We divided the normal distribution into 16 parts. Consequently, we got 4 bits of random information as $2^4 = 16$. So far, our generator produces 4 Mbit/s. We can improve the speed of the generator in two ways. The first way is the increasing of the density of the division, the second is the increase in the repetition rate of the laser signal. I verified the quality of the generated random bits using the dieharder tests. The results can be found in the appendix A in Tab. A.1. All tests passed successfully, except two results of the test which were granted as WEAK. It is because we do not have enough numbers to test in data sample.

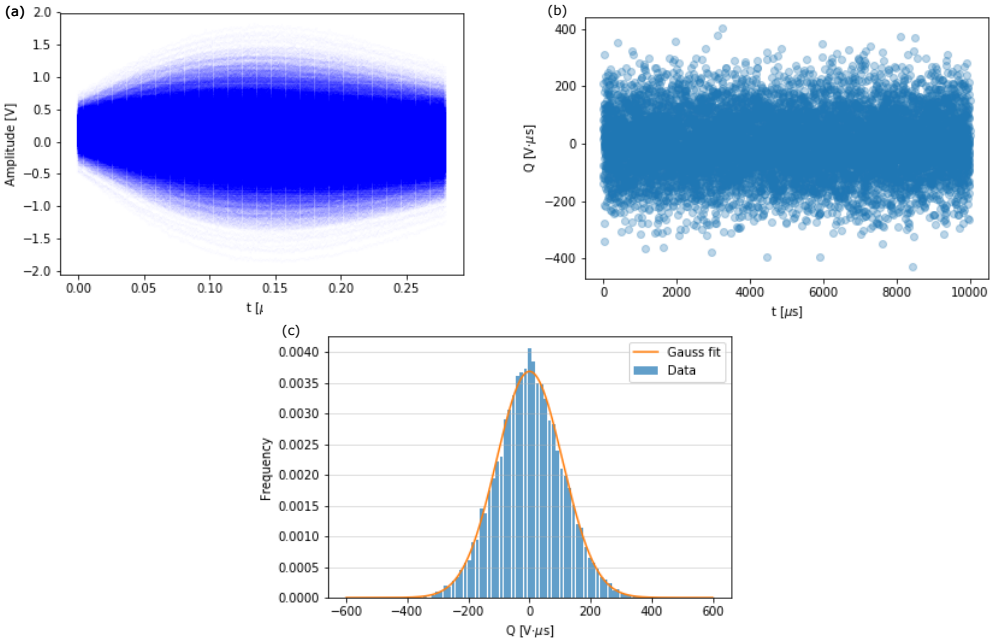

Figure 5.4: Results of measurement with power of local oscillator $N_{LO} \approx 651$ mio photons in the entry. This result is no longer in linear region, but in comparison with Fig. 5.3, there is growth of the variance. (a) Every pulse of the one measurement visualized one over another. (b) Amplitude of quadratures visualized over time. (c) Histogram made from quadratures, fitted with Gauss distribution.

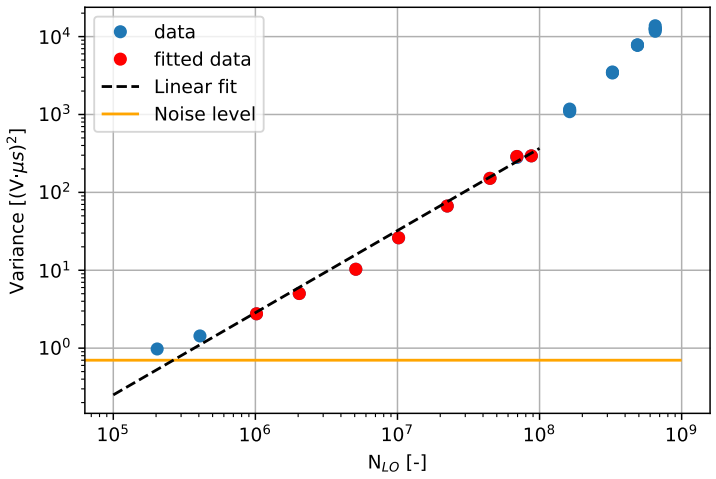

Figure 5.5: The variance of the quadratures against the intensity of LO. Plot is LogLog scaled. Linear interval is between 1 mio - 100 mio photons (red points). The yellow line shows the electronic noise level.

Chapter 6

Conclusions and outlook

As shown in this thesis, the homodyne detection is a powerful tool not just in quantum state reconstruction but also in other fields of quantum physics. It is useful to have a well performing homodyne detector for the reconstruction of the quantum state. In the first chapter, I explained the fundamentals of homodyne detection. In the second chapter, I measured parameters, as the gain, which was $g = 9.1\ \mu\mathrm{V}/e^{-1}$ and electric noise of the our homodyne detector which was only 300 electrons on the input. This detector was shown to be sufficient for measuring the quantum noise. I determined the working region of the amplifier and its response. In the third chapter, I measured the response and the quantum efficiency of the photodiodes. Also, I measured the response of the photodiodes on the U_{bias} and I found out quantum efficiency of photodiodes on the incoming polarization. I made an analysis and chose the best pair of photodiodes for use in our detector. After completion of the detector, I made the first optical measurement. It was the measurement of the vacuum state. I measured quantum noise of vacuum state of light and I found the quadrature distribution. I measured the variation of the vacuum state for a different power of local oscillator. With this measurement, I found out limits of our homodyne detector. The clearance is larger than 23 dB. As the final result, I processed the quadrature data and I made the quantum random number generator, which passed the dieharder random number tests. Our quantum random number generator was able to produce 4 of random megabits per second. The speed of this generator can be further increased.

Our next step will be the improvement of the quantum random number generator. We want to increase the bit rate. We will also improve its quality using various randomness extractors, such as Von Neumann extractor. We will build a new homodyne detector based on a trans-impedance amplifier with faster response. If the bandwidth of the detector will be large enough (> 80 MHz), we would like to use it with a signal from Ti:Sapphire laser. I want to use such detector to measure quantum states of light. Furthermore, I will use algorithms for quantum tomography to estimate quantum features of multi-photon states and other highly non-classical states.

Bibliography

[1] R. E. Slusher, L. W. Hollberg, B. Yurke, J. C. Mertz, and J. F. Valley, "Observation of squeezed states generated by four-wave mixing in an optical cavity," *Phys. Rev. Lett.*, vol. 55, pp. 2409–2412, 1985.

[2] D. Smithey, M. Beck, and M. G. Raymer, "Measurement of the Wigner distribution and the density matrix of a light mode using optical homodyne tomography: Application to squeezed states and the vacuum," *Physical review letters*, vol. 70, no. 9, 1993.

[3] H. Hansen, *Generation and characterization of new quantum states of the light field*. PhD dissertation, Konstantz University, 2000.

[4] R. Okubo, M. Hirano, Y. Zhang, and T. Hirano, "Pulse-resolved measurement of quadrature phase amplitudes of squeezed pulse trains at a repetition rate of 76 mhz," *Opt. Lett.*, vol. 33, no. 13, pp. 1458–1460, 2008.

[5] R. Kumar, E. Barrios, A. MacRae, E. Cairns, E. H. Huntington, and A. I. Lvovsky, "Versatile wideband balanced detector for quantum optical homodyne tomography," *Optics communications*, vol. 285, pp. 5259–5267, 2011.

[6] A. Zavatta, M. Bellini, P. L. Ramazza, F. Marin, and F. T. Arecchi, "Time-domain analysis of quantum states of light: noise characterization and homodyne tomography," *J. Opt. Soc. Am. B*, vol. 19, no. 5, pp. 1189–1194, 2002.

[7] O. Haderka, V. Michálek, V. Urbášek, and M. Ježek, "Fast time-domain balanced homodyne detection of light," *Appl. Opt.*, vol. 48, no. 15, pp. 2884–2889, 2009.

[8] A. Ourjoumtsev, R. Tualle-Brouri, J. Laurat, and P. Grangier, "Generating optical Schrödinger kittens for quantum information processing," *Science*, vol. 312, 2006.

[9] M. Avesani, D. G. Marangon, G. Vallone, and P. Villoresi, "Source-device-independent heterodyne-based quantum random number generator at 17 Gbps," *Nature Communications*, vol. 9, no. 1, p. 5365, 2018.

[10] H. Hansen, T. Aichele, C. Hettich, P. Lodahl, A. I. Lvovsky, J. Mlynek, and S. Schiller, "Ultrasensitive pulsed, balanced homodyne detector: application to time-domain quantum measurements," *Opt. Lett.*, vol. 26, no. 21, pp. 1714–1716, 2001.

[11] P. J. Windpassinger, M. Kubasik, M. Koschorreck, A. Boisen, N. Kjærgaard, E. S. Polzik, and J. H. Müller, "Ultra low-noise differential ac-coupled photodetector for sensitive pulse detection applications," *Measurement Science and Technology*, vol. 20, no. 5, p. 055301, 2009.

Appendix A

Statistical tests

Table A.1: Results of Dieharder tests of randomness of our generator. In case of multiple tests, the smallest p-value was chosen.The tests were applied to 10 000 4bit numbers generated from 10 000 quadrature values measured by the developed homodyne detector.

dieharder version 3.31.1 Copyright 2003 Robert G. Brown					
test name	ntup	tsamples	psamples	p-value	Assessment
diehard birthdays	0	100	100	0.21497146	PASSED
diehard operm5	0	1000000	100	0.14241201	PASSED
diehard rank 32x32	0	40000	100	0.60546573	PASSED
diehard rank 6x8	0	100000	100	0.24139853	PASSED
diehard bitstream	0	2097152	100	0.74073273	PASSED
diehard opso	0	2097152	100	0.20538212	PASSED
diehard oqso	0	2097152	100	0.48751682	PASSED
diehard dna	0	2097152	100	0.72747834	PASSED
diehard count 1s str	0	256000	100	0.13006773	PASSED
diehard count 1s byt	0	256000	100	0.00340306	WEAK
diehard parking lot	0	12000	100	0.50228590	PASSED
diehard 2dsphere	2	8000	100	0.11097490	PASSED
diehard 3dsphere	3	4000	100	0.29285974	PASSED
diehard squeeze	0	100000	100	0.97151958	PASSED
diehard sums	0	100	100	0.29766412	PASSED
diehard runs	0	100000	100	0.99260417	PASSED
diehard runs	0	100000	100	0.34179895	PASSED
diehard craps	0	200000	100	0.98341518	PASSED
diehard craps	0	200000	100	0.68555885	PASSED
marsaglia tsang gcd	0	10000000	100	0.06557901	PASSED
marsaglia tsang gcd	0	10000000	100	0.25595429	PASSED
sts monobit	1	100000	100	0.66552170	PASSED
sts runs	2	100000	100	0.95157186	PASSED
sts serial	16	100000	100	0.18019484	PASSED
rgb bitdist	8	100000	100	0.02811108	PASSED
rgb minimum distance	3	10000	1000	0.27427811	PASSED
rgb permutations	4	100000	100	0.49329694	PASSED
rgb lagged sum	31	1000000	100	0.00273749	WEAK
rgb kstest test	0	10000	1000	0.60186049	PASSED
dab bytedistrib	0	51200000	1	0.03584510	PASSED
dab dct	256	50000	1	0.79110916	PASSED
dab filltree	32	15000000	1	0.33912115	PASSED
dab filltree2	1	5000000	1	0.57657326	PASSED
dab monobit2	12	65000000	1	0.57781143	PASSED